ABSTRACT

Title of Thesis:	EXPERIMENTAL STUDY OF MICROENCAPSULATED PHASE CHANGE SLURRY IN SHELL-AND-TUBE HEAT EXCHANGER
	Akshaya Sridhar, Master of Science, 2026
Thesis Defense Directed by:	Dr. Damena Agonafer Department of Mechanical Engineering

Microencapsulated phase change slurry (MPCS) can release and store heat during phase transitions, allowing for a thermal energy transfer to occur when the core material transitions between solid and liquid phases. Numerical and experimental research has shown that MPCS slurries, using water as a base fluid, can improve thermal performance. To investigate the use of MPCS as a working fluid, this study considers slurry synthesis, characterization, and experimental investigation of the MPCS in a shell-and-tube heat exchanger. Characterization of the slurry was performed through thermal analysis, rheometry, and zeta potential measurements. The heat transfer performance and pressure drop across the heat exchanger were benchmarked against a baseline case of water. The effect of particle concentration and Reynolds number on the heat transfer performance of the slurry were evaluated. The results indicate that particle concentration improves heat transfer performance but also increases the pumping requirements due to the increase in viscosity along with particle concentration. The maximum average heat transfer coefficients of 5% and 7.5% mass fraction MPCS was 16.7% and 21.6% higher, respectively, than that of water under the same conditions. Pressure drop increased by 288.1% and 321.2% compared to water for 5% and 7.5% MPCS respectively. A performance enhancement criterion (PEC) was utilized to compare gains in heat transfer performance with increases in pumping power. Despite higher heat transfer coefficients (HTC) at greater Reynolds numbers, water had superior thermo-hydraulic performance at Re > 1550 due to lower residence times and increased pumping power required for the slurries.

EXPERIMENTAL STUDY OF MICROENCAPSULATED PHASE CHANGE SLURRY IN

SHELL-AND-TUBE HEAT EXCHANGER

by

Akshaya Sridhar

Thesis submitted to the Faculty of the Graduate School of the
University of Maryland, College Park in partial fulfillment
of the requirements for the degree of
Master of Science
2026

Advisory Committee:
Professor Damena Agonafer, Chair/Advisor
Professor Francis Patrick McCluskey
Professor Amir Riaz

Table of Contents

List of Figures

Chapter 1 Introduction

1.1 Phase Change Materials

Phase change materials (PCMs) are a type of material that uses latent heat during phase transition to store and release thermal energy. PCMs possess the unique ability to absorb and release large quantities of heat without rapid increase in temperature when they change state, providing their unique use-case in thermal management applications. Phase change materials typically undergo solid-liquid transformations, storing and releasing thermal energy as they transition between phases. Materials employed for PCMs exhibit high latent heat and possess a melting temperature within the range of the relevant application. Relevant materials which have been studied over the past 40 years are hydrated salts, paraffin waxes, fatty acids, and eutectics [1]. Among the various options, PCMs are broadly classified into organic and inorganic materials, with organic PCMs further divided into paraffin and non-paraffin types. Organic materials are favorable due to their non-corrosivity and stability [1]. Additionally, paraffin waxes are the most economical, and provide thermal energy storage density, but low conductivity [2]. The high latent heat of fusion intrinsic to PCMs allows for higher energy density, higher specific heats and temperature stability in a small area [3]. Solid-liquid phase change material undergoes three different phases as described by Tan et al [2]. In the first phase, the solid material reaches a state where the ambient temperature is the melting temperature. In the second phase, the solid PCM melts under a constant melting temperature, and the latent heat is stored. In the last phase, the liquid PCM rises in temperature as sensible heat energy is stored in the liquid. PCMs are capable of storing 5-14 times more latent heat per unit volume than sensible heat storage materials (e.g. water) [1]. The selection of an appropriate PCM depends on the application temperature, the latent heat required, stability of the PCM, low subcooling, and low volume change. Reproducible phase change, which allows for the cyclic storage release and absorption of latent heat is also desired [4].

To increase heat transfer area, reliability and supplement existing working fluids, polymeric containers for PCM using encapsulation technology have been employed. These capsules, micrometers in size, are referred to as microencapsulated phase change material (MEPCM), and consist of a polymeric shell and PCM as the core material. With microencapsulation technology, the MEPCM shell prevents contact of the PCM with the surrounding environment and provides a large variety of applications for the PCM [5].

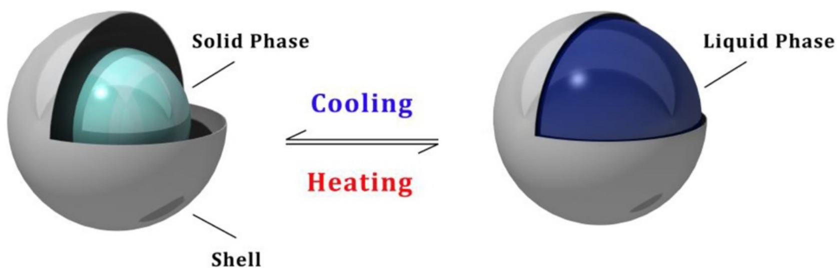

Figure 1.1 Schematic of microencapsulated phase change material [6]

When MEPCM is dispersed in a carrier fluid, a two-phase suspension is formed, known as microencapsulated phase change slurry (MPCS). The introduction of a carrier fluid allows for a higher degree of convective heat transfer from fluid-particle interaction. The phase change and latent heat increase the effective specific heat of the working fluid result in heat transfer enhancement [7]. Kasza and Chen [8] were one of the first to propose phase change slurries, with particles just under 1 mm, for the enhancement of solar energy and waste heat storage and investigated the possibility of an increase of heat transfer coefficients over a single-phase working fluid. Alvarado et al. [9]found that the slurry effective heat capacity increased by 40% compared to water in identical flow conditions, using a 7% wt. n-tetradecane slurry in a heat transfer loop. However, heat transfer coefficients of the MPCS are typically lower than that of water with the same velocity, which was attributed to the attenuation of turbulence. Charunyakorn et al. [10] found that in MPCS slurry flow with forced convection, the Stefan number and particle concentration are the most important variables in terms of improving the heat transfer coefficient, and found a 1.5x to 4x improvement over water under ideal conditions. Wang et al. [11] found that the Reynolds number and slurry mass fraction dominated heat transfer performance for organic MPCS in a circular tube. Enhanced heat transfer performance was achieved for slurries with concentrations of both 5% and 10%, with an increase of 1-2.5x times higher average Nusselt number compared to plain water. It was found that a lower heat transfer coefficient was found for the 10% slurry, compared to the 5% slurry, which was attributed to the suppression of turbulence. It was found in some cases; the 10% slurry approached the heat transfer coefficient of water at flow conditions with a low Reynolds number. Zhao et al. [12] found that a three-fold increase in the bulk Stephan numbers reduced heat transfer enhancement ratio by 30%. Particle concentration and the Stephan number were the most important parameters. Shaukat et al. [13] found that at Reynolds numbers of Re = 1200, the average Nusselt number was found to be 12.1% and 28.3% higher than pure water for concentrations of 5% and 10% MEPCM respectively. It was found that when the temperature of the hot water entering the heat exchanger increased, increasing the Stefan number, the heat transfer coefficient of the slurry dropped. It was also found that the pressure drop increases with respect to flow rate and mass concentration of the PCM. Kuravi et al. [14] conducted heat transfer experiments of water-based MPCS within a microchannel test set-up. In the experiments, it was shown that as the flow rate of the slurry increased, the heat transfer coefficient also increased. However, the heat transfer coefficient of the slurry was lower than that of water. This was attributed to low thermal conductivity of water and incomplete melting of the PCM. As seen in experiments by Shaukat et al., it was theorized that with higher inlet flows, the particles did not have sufficient time to achieve melting in the heated region. Additionally, it was theorized that larger PCM particles would require slower flow rates in order to achieve as much melting as smaller particles. At this point, few experimental studies have been performed with MPCS as a working fluid in heat exchangers, especially tube-in-tube or shell-in-tube. This gap in research underscores the need to investigate the behavior of MPCS in an experimental context for this type of geometry. This experiment aims to further characterize the physical attributes of MPCS and its performance as a working fluid within a shell-and-tube heat exchanger.

1.2 Heat Exchanger Design

Heat exchangers are used to transfer enthalpy between two or more fluids and are used in both heating and cooling. Basic types of heat exchangers include shell-and-tube heat exchangers, double pipe heat exchangers, and plate heat exchangers. Other types of heat exchangers are created on a smaller scale, including minichannels and microchannels. A shell-and-tube heat exchanger consists of a "shell", which contains tubes inside. One fluid flows within the tubes, and the other fluid will flow in the shell surrounding the tubes. Heat is transferred from one fluid to another through the tube walls. In a U-tube heat exchanger, the tubes are bent within the shell, in the shape of a "U". In parallel flow of a heat exchanger, two fluids enter through inlets located on the same side and exit through outlets on the same side as well. In counterflow, fluids enter from opposing sides of the heat exchanger. The counterflow design is considered to be the most efficient and can transmit the most heat per unit mass as the average temperature difference across any unit length is higher [15]. A double pipe heat exchanger, represented in Figure 1.2, is a more simple design compared to the shell-and-tube, and consists of two concentric pipes, where the "tube" pipe is within the "shell" pipe.

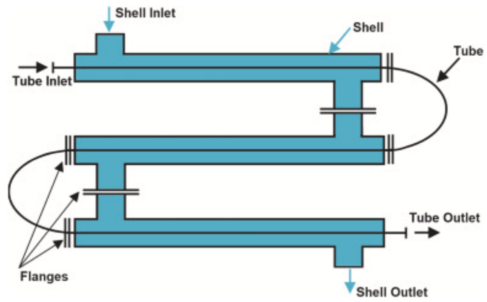

Figure 1.2 Schematic of a double-pipe heat exchanger [16]

Higher tube-side inlet velocity results in a higher Reynold's number, which can improve heat transfer performance. However, the square of velocity is directly related to pressure drop along the tube side, which can increase the need for pumping power [17]. For turbulent flows, the tube-side heat transfer coefficient varies to the 0.8th power of the tube-side mass velocity [18].

Heat exchanger effectiveness can be quantified by the ratio of heat actually transferred from the intended fluid and the maximum heat that can be transferred. The heat transfer rate is governed by the following equation:

$$\dot{Q} = \dot{m}C_{p,w}\left(T_{w,i} - T_{w,o}\right) \tag{1.1}$$

The heat capacity, $C_{p,w}$, of the working fluid within a heat exchanger is critical to the amount of heat transferred and therefore impacts the effectiveness of the heat exchanger. By increasing the heat capacity of the working fluid, the heat transfer rate and effectiveness of the heat exchanger can be increased. The use of MPCS in a double-tube heat exchanger has been explored to increase heat transfer performance [19]. The addition of the MPCM particles allows for heat to be absorbed in both the sensible and latent forms, whereas plain water as a working fluid can only utilize sensible heat.

1.3 Key Issues

Several logistical difficulties have been identified with the use of MPCS, including low thermal conductivity, increased pumping power due to higher viscosities, and stability of the properties under the strain of thermal cycling.

Supercooling of MEPCM leads to lower crystallization temperature, which in turn reduces the temperature at which latent heat will be released, and the PCM does not solidify at the freezing temperature. This can cause challenges in heat transfer issues, as large temperature differentials can be required within the application to absorb and release latent heat [20].

Clogging and agglomeration are also concerns with MPCS. The separation of the MEPCM from the base fluid can occur due to density differences between the particles and the fluid. The potential rupture of PCM shells can also contribute to clogging and increase the pumping power requirement.

The increase of particle concentration of the slurry also increases the pressure drop and pumping requirements. Chen et al. [21] found a pressure drop increase of 13.4% with 1% weight MEPCM in slurry compared to water at the same Reynolds number. The increase in flow resistance is caused by the increase in slurry viscosity from microcapsules. Figures of merit have been developed to compare the benefits of the increase in heat transfer compared to the pressure drop and increasing pumping requirement for slurries.

1.4 Objective

This study aims to characterize the physical and thermal properties of Microencapsulated Phase Change Slurry (MPCS) and investigate the performance of the slurry as a working fluid for the shell-and-tube heat exchanger design. It is hypothesized that the addition of MPCS as a working fluid will increase the heat transfer performance and effectiveness of the shell-and-tube heat exchanger compared to the use of plain water as a working fluid. The thermal and physical properties of the phase change slurry will be characterized. Viscosity is measured to understand the impact of concentration of microcapsules within the slurry. Additionally, the stability of the slurry is analyzed to improve reliability and avoid clogging. This study considers the effect of slurry PCM concentration on heat transfer performance for the shell-and-tube heat exchanger, and compares the results to water, the baseline working fluid to assess improvement. The pressure drop across the heat exchanger is analyzed to understand the costs of increased pumping power requirements. A Performance Enhancement Criteria (PEC) is used to analyze the potential benefits in heat transfer performance to the pumping requirement. The findings of this study provides insight on MPCS synthesis and the effectiveness of MPCS in shell-and-tube heat exchangers for thermal management applications.

Chapter 2 Slurry Characterization and Synthesis

2.1 Slurry Synthesis

The MEPCM referenced in this study is Nextek 37D and consists of a paraffin core with a melamine shell. An SEM image of Nextek 37D particles is shown in Figure 2.1.

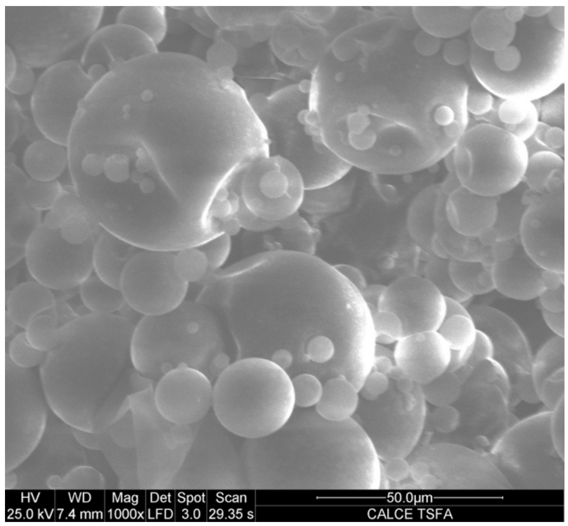

Figure 2.1 SEM image of Nextek 37D

The MEPCM referenced in this study is Nextek 37D and consists of a paraffin core with a melamine shell. The melting point of Nextek 37D is 37°C, and the particle size is 15-30 microns. The MEPCM particles were added to deionized water along with sodium lauryl sulfate, an anionic surfactant. This mixture was ultrasonicated for 15 minutes. Slurries of mass concentrations ranging from 2.5% to 7.5% were synthesized. Thermophysical properties of the slurry were measured using DSC, rheometry, and zeta potential analysis.

2.2 Thermal Characterization

The thermal properties of Nextek 37D were analyzed using differential scanning calorimetry (DSC). The resulting DSC curves are displayed in Figure 2.2.

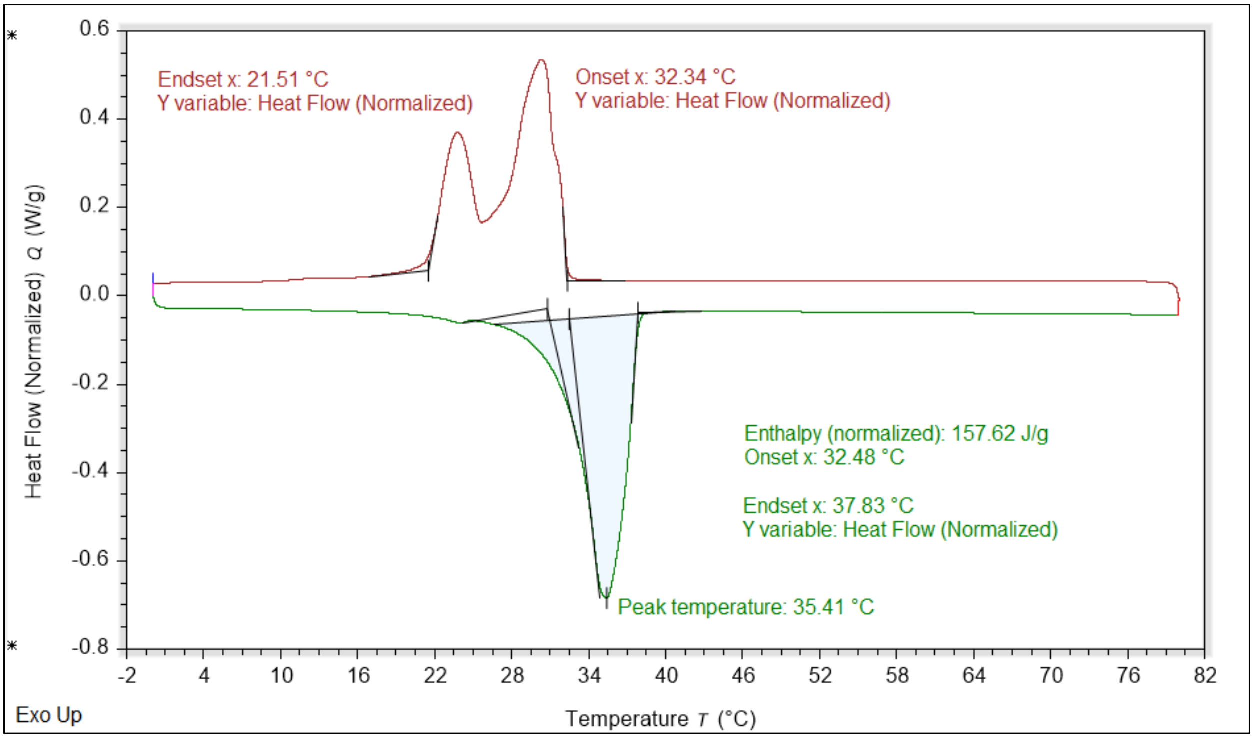

Figure 2.2 Differential scanning calorimetry curve of Nextek 37D

It was observed that the particles begin to melt at 32°C, and the end of melting occurred at 38°C. The latent heat measured from the DSC measurements is 157.6 J/g. As seen in Figure 2.1, supercooling occurred for Nextek 37D and solidification occurs at 21.5 °C, as indicated in Figure 2.2. This refers to a phenomenon where phase change material remains in its liquid state at temperatures lower than the solidus temperature [22].

2.3 Viscosity

Five different samples were created to examine the effect of MEPCM concentration on the viscosity of a slurry. The samples consisted of 2.5%, 5%, 7.5% and 10% mass fraction MEPCM, along with pure distilled water, with no surfactant added. The rheology of these samples was measured using a TA Instruments ARES-G2 Rheometer equipped with a cup and bob geometry using rotational shear. Each sample was placed in the cup, and the bob was lowered into the sample. The bob rotates within the cup, and the torque which is required to rotate the bob at a particular speed is measured. This data is then used to calculate the viscosity of the fluid when steady flow is reached. The temperature of the samples was standardized to 25°C before measurement. Viscosity was recorded for shear rates of 0 through 200 s^{-1}.

Viscosity has an important role in the pressure drop of the slurry within the manifold, resulting in higher pumping requirements. Literature shows a relationship between the increased mass fraction of the slurry and viscosity. Delgado et al. [23] observed slurry with a 14% PCM microcapsule fraction had a viscosity approximately five times of water, whereas a 20% and 30% microcapsule mass fraction was 6 times higher and 18 times higher respectively. Zhang and Zhao examined rheological behaviors of various slurries and determined that the shear stress increased linearly and could be considered a Newtonian fluid for MEPCS with a microcapsule mass fraction under 25% [24]. In a study by Rutgers comparing several models for the viscosity of spheres in Newtonian liquids, nearly all models reported Newtonian flow up to a volume fraction of 25% particle [25]. Multiple other studies show Newtonian behavior with lower PCM concentrations, and shear-thinning behavior at higher concentrations [23], [26]. Delgado explains that at high shear rates, the microcapsules begin to form layers where the average distance between particles decreases in the direction of the flow and increases the direction perpendicular to flow. This change makes it easier for the fluid to move and decreases the viscosity. It can also be observed that rotational tests of liquids with low viscosity can create secondary flows, increasing the measured viscosity. Figure 2.3 displays the effect of particle concentration on the viscosity of the slurry. Increases in the slurry viscosity are observed with increasing volumetric concentration. Additionally, in Figure 2.4, the experimental data is plotted against various viscosity models.

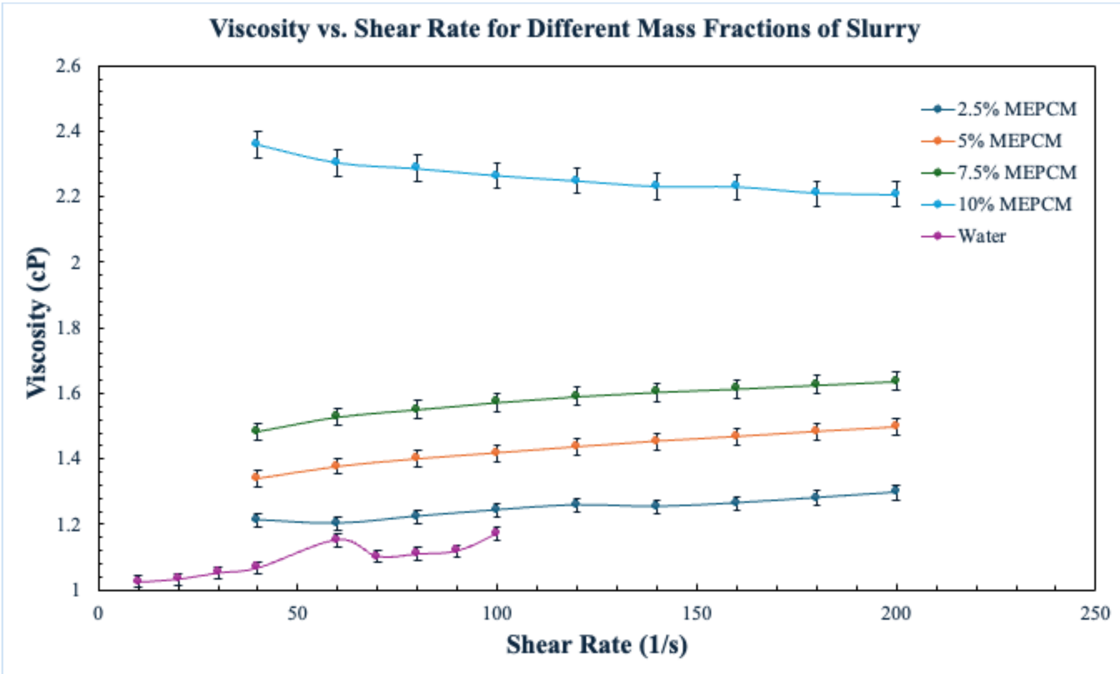

Figure 2.3 Variation in slurry viscosity with particle concentration

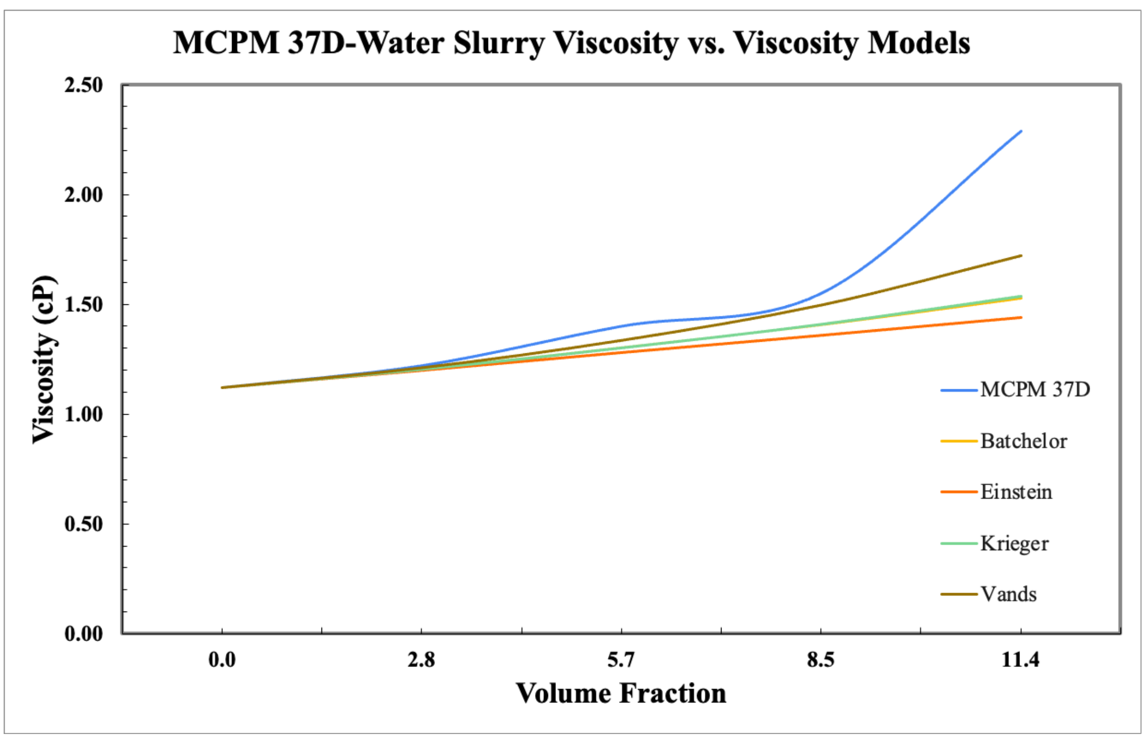

Figure 2.4 Viscosity models compared to experimental data

Selvakumar et al. [27] discuss various viscosity models. Einstein's model is most effective for volume fractions less than or equal to 0.01. Batchelor's model builds onto Einstein's by considering Brownian motion among particles where volume fraction is less than or equal to 0.1 Krieger and Dougherty proposed a correlation for concentrations above 0.1, to attribute to the non-Newtonian behavior of suspensions. For lower concentrations, and lower shear rates, it can be seen that the slurry behaves as a Newtonian fluid. The fluid can then be described using the Vand equation, which can predict viscosity at particulate volumetric concentrations below 37% [28]. The Vand equation is given below:

$$\frac{\mu_s}{\mu_f} = (1 - \phi - A\phi^2)^{-2.5} \tag{2.1}$$

Where μ_s is the effective viscosity of the slurry, ϕ is the volumetric fraction of the particles, μ_f is the viscosity of the base fluid, and A is a constant, which depends on the size and shape of the particle. Vand initially used $A = 1.16$ for glass spheres with a diameter of 0.013 cm [29]. Mulligan et al. [30] developed the value $A = 3.4$ for a slurry with microencapsulated PCM particles of 10-30 μm diameter.

2.4 Stability

PCM slurries are subject to several instability problėms. The creaming phenomenon is characterized by a difference in density between buoyant particles and the liquid in a suspension [31]. Due to the lower specific gravity of the MPCM 37D particles, the MPCM floats to the surface when added to water. Additionally, flocculation and the agglomeration of particles is another possibility [32]. Typically, surfactants have been used to improve the stability of MEPCM slurries.

Surfactants reduce tension between the microcapsules and the aqueous phase [33]. Lin et al. [34] demonstrate that surfactant can improve stability of MEPCM slurries through a wide range of microcapsule concentrations. The addition of surfactants which can bind to the microcapsule walls can create repulsion between particles and therefore promote stability.

The NanoBrook Omni Particle Size and Zeta Potential Analyzer was used to measure stability trends in PCM and PCM concentration. Zeta potential refers to the electric potential between the boundary between the diffuse region of a particle, and the bulk fluid. The diffuse region of a particle refers to the outer layer which contains the inner Stern layer. Within the Stern layer, ions are strongly bound to a particle, and in the outer diffuse region, the ions are weakly associated with the particle. When a particle moves throughout the fluid, ions in the diffuse and Stern layer within a certain boundary move along with it. The zeta potential represents the stability of the mixture. If the zeta potential is highly positive or negative, the particles will repel one another, and it is less likely for the particles to clump together. Zeta potential close to zero indicates low repellence between particles and a higher possibility for agglomeration; therefore, a highly negative or highly positive zeta potential is ideal. In these experiments, Sodium Lauryl Sulfate (SLS) from Crafter's Choice was added to the MPCM-water slurry to improve stability. SLS is an anionic surfactant, and was recommended by the particle manufacturer as it would bind best with the microcapsule wall, as the melamine resin is positively charged. Therefore, it is expected that the zeta potential will be negative.

The zeta potential of three samples of MPCM slurry were measured at $c = 0.5\%$, 1%, and 2% using the NanoBrook instrument, while surfactant percentage was held constant. The zeta potential decreased with increasing MPCM concentration, indicating that higher concentrations will have a higher degree of particle-particle interactions and lower stability. Figure 2.5 shows the experimental results of increasing the particle mass fraction and zeta potential.

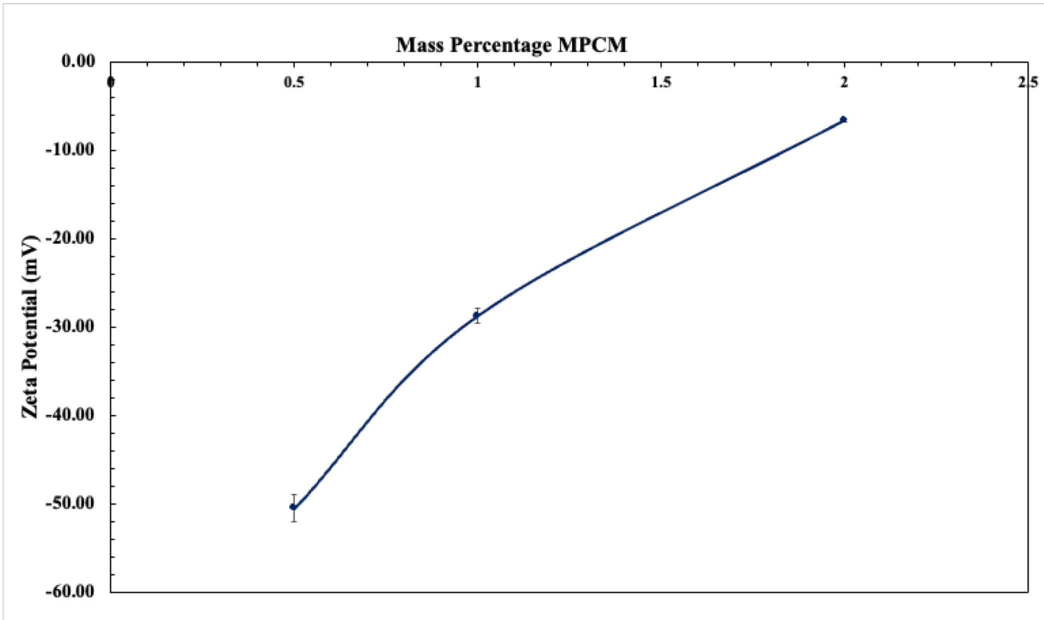

Figure 2.5 Variation of zeta potential with PCM concentration

Additionally, the mass percentage of MPCM within the slurry was held constant, and various concentrations of SLS were measured in the NanoBrook instrument. As shown in Figure 2.6, the zeta potential is largest when the SLS is 0.25% weight surfactant to weight MPCM.

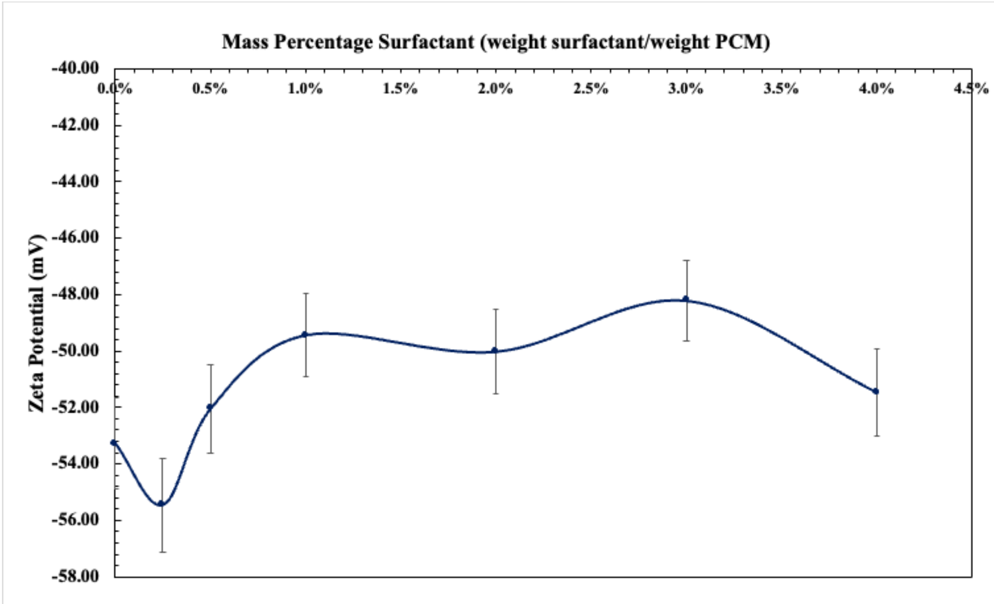

Figure 2.6 Variation in zeta potential with surfactant at constant MPCM concentration

As the percentage of surfactant increased past 0.25%, the zeta potential of the slurry approached zero, indicating a higher degree of instability. In this case, a higher degree of stability is indicated by a more negative zeta potential. This indicates that the particles are more likely to repel one another.

Chapter 3 Experimental Methodology

3.1 Flow Loop Design

A schematic of the flow-loop is shown in Fig. 3.1. The working fluid is held in a reservoir and circulated throughout the tubing using a peristaltic pump. The working fluid is preheated to a temperature equal to the solidus point of the MEPCM, as it flows through a coil placed in a thermostatic bath. The slurry is then pumped through the tubes of the shell and tube heat exchanger. The heat exchanger is wrapped in fiberglass to insulate the manifold and control heat loss to the environment. RTDs and T-type thermocouples have been placed in the inlet and outlet tubes of the slurry and the hot water side, respectively, to record temperature continuously. Mixing was employed in both the chiller and the preheater thermostatic bath to improve heat transfer. An Omega PX409 differential pressure transducer was connected to both the inlet and outlet slurry tubes using valves. The heated slurry exits the heat exchanger and passes through another coil placed in a chiller to bring the temperature down past the point of MEPCM solidus temperature and the supercooling point, 32°C and 21.5°C, respectively, from where it is then pumped back into the reservoir. On the hot water side of the loop, a submersible pump is placed into a thermostatic bath to maintain a constant temperature. The water is pumped through a flow meter, and into the shell of the heat exchanger. Once exiting the heat exchanger, the hot water is pumped back through the thermostatic bath. Likewise, the inlet and the outlet of the hot water are measured using thermocouples. All measured quantities were logged using a data acquisition system. After several minutes of steady state temperatures, data was recorded for each experiment for about 5 minutes and the data is averaged to get final data points.

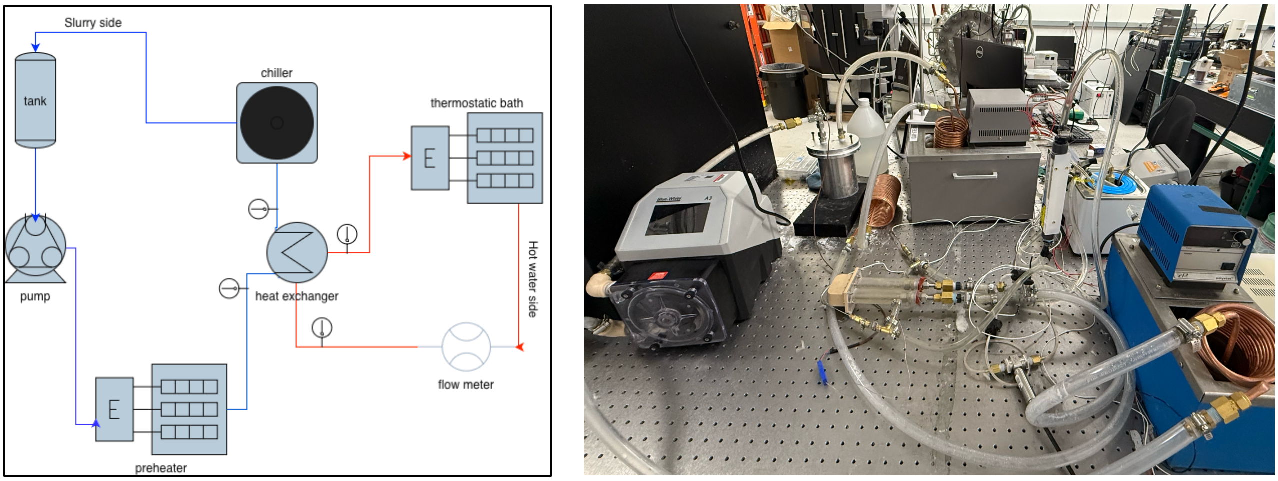

Figure 3.1 Flow Loop Set-up

In Fig. 3.1, thermocouples are marked where readings were recorded at the slurry and hot water inlet and outlets.

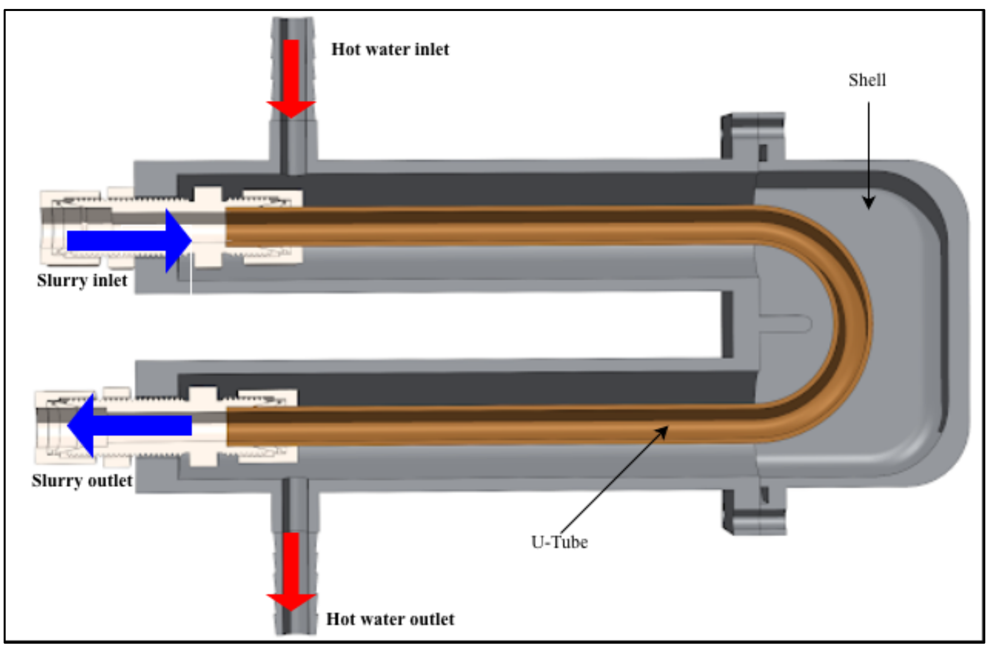

Figure 3.2 Cross-section diagram of test section manifold in parallel flow configuration

The test device is a U-tube shell-and-tube heat exchanger. The U-tube consists of a steel tube that is 0.36 m and has an inner diameter of 0.704 cm. Slurry enters the U-tube through plastic tubing. The shell consists of two plastic tubes connected to a 3D printed piece, fully encasing the U-tube. The shell is connected to the tubing which supplies hot water through T-joints.

3.2 Flow Loop Parameters

Three different mass fractions were tested, along with pure water as a baseline. The mass fractions were 5%, and 7.5%. Literature shows that with the increase of mass fraction of the PCM, the heat capacity of the slurry also increases due to the contribution of latent heat [35]. On the hot-water side of the loop, the inlet temperature was held constant at 40°C, to remain close to the melting range of the MPCM. Additionally, the slurry inlet temperature was preheated to 32°C, which is the beginning of the melting range for the particles in this study.

Three different Reynolds numbers were held constant for each of the slurries (Re = 750, Re = 1550, and Re = 1930). The flow rate of the slurry varied using the settings of the peristaltic pump. Previous literature shows that the increase in fluid velocity increases the heat transfer performance of MEPCM slurries, as a result of greater momentum transfer [36].

In a single pass heat exchanger, the coolant and the hot-side fluid are exposed to each other once. Parallel flow describes where the inlet is on the same side of the heat exchanger for both fluids (hot water and slurry). Counterflow marks where the inlet of one fluid is on the same side where the other one will exit. Both counterflow and parallel flow were tested for each test condition. For each configuration (parallel or counterflow), three tests were performed at Re = 750, Re = 1550, and Re = 1930 respectively. In total, this amounted to six tests per mass fraction, or 18 tests in total.

3.3 Data Reduction

From the RTDs placed in the inlet and outlet of both the slurry and the hot water side of the heat exchanger, several values can be derived to investigate the heat transfer performance. The temperatures on both the inlet and outlet of the hot side of the heat exchanger are denoted by T_w, with $T_{w,i}$ and $T_{w,o}$ representing the inlet and outlet respectively. Likewise, the temperatures on the inlet and outlet of the slurry side are represented by $T_{s,i}$ and $T_{s,o}$. The volumetric flow rate of both the slurry ($\dot{Q}_s$) and water ($\dot{Q}_w$) are both recorded from the pump readings and hot water flow meter respectively. Additionally, the pressure drop across the slurry tube inlet and outlet are denoted as ΔP. The average heat rate dissipated by the hot water is then derived as:

$$Q = \dot{m}_w C_{p,w}\left(T_{w,i} - T_{w,o}\right) \tag{3.1}$$

Where $\dot{m}_w$ is the mass flow rate of the water, calculated from the volumetric flow rate, and $C_{p,w}$ is the heat capacity of water. The heat loss was corrected for heat loss to the environment. This was done by running the hot water through the loop with no slurry present, to observe the temperature drop resulting from heat absorption by the environment. The corrected heat loss was then calculated by subtracting the heat loss from the environment by the average heat rate dissipated during the slurry experiments. Using the adjusted heat loss, effective heat capacity of the slurry is calculated as:

$$C_{p,s} = \frac{Q}{\dot{m}_s\left(T_{s,o} - T_{s,i}\right)} \tag{3.2}$$

With the assumption that all heat loss can be attributed to the coolant. Where $\dot{m}_s$ represents the mass flow rate of the slurry. The logarithmic-mean temperature difference represents the log-mean temperature difference between the hot and cold fluid flows, and is calculated as:

$$\Delta T_{LMTD} = \frac{\Delta T_1 - \Delta T_2}{\ln\left(\frac{\Delta T_1}{\Delta T_2}\right)} \tag{3.3}$$

In parallel flow, $\Delta T_1 = T_{w,i} - T_{s,i}$ and $\Delta T_2 = T_{w,o} - T_{s,o}$.

For counterflow, $\Delta T_1 = T_{w,i} - T_{s,o}$ and $\Delta T_2 = T_{w,o} - T_{s,i}$.

From this, the overall average heat transfer coefficient, or the conduction-convection resistance between hot and cold fluids [37], is calculated as:

$$UA = \frac{Q}{\Delta T_{LMTD}} \tag{3.4}$$

Performance enhancement criterion (PEC) can be derived, which is used to compare the performance of water and slurry as coolants [38] :

$$PEC = \frac{U_s/U_w}{\left(\Delta P_s/\Delta P_w\right)^{\frac{1}{3}}} \tag{3.5}$$

The PEC evaluates the thermal performance of slurry compared to water as a working fluid, considering the increase in pressure drop, and therefore pumping power. This performance ratio is commonly used in the evaluation of multi-tube heat exchangers.

3.4 Uncertainty Analysis

The temperature reading errors from the thermocouples is equal to 0.1°C. The error generation by the Omega PX409 pressure transducer is ±0.08%. The hot water flow rate was read by a rotameter, which has an error of 2.5%. Based on the formula for the heat flux, where the inlet and outlet temperatures are measured. The error propagation variance formula is as follows:

$$s_f = \sqrt{\left(\frac{\partial f}{\partial x}\right)^2 s_x^2 + \left(\frac{\partial f}{\partial y}\right)^2 s_y^2 + \cdots} \qquad (3.6)$$

Where f represents a derived value, and x represents a directly measured value.

Chapter 4 Results and Discussion

For each mass fraction (c=0%, c = 5%, and c = 7.5%), twelve experimental runs were performed. Three tests at various slurry flow rates were performed at T = 40°C. This was repeated for the other configuration of the heat exchanger (counterflow and parallel). Heat transfer data was collected for a minimum of five minutes once steady state was achieved for all conditions.

4.1 Heat Transfer Performance and PCM Concentration

The heat transfer coefficient was calculated for each inlet condition and mass concentration, as displayed in Figure 4.1.

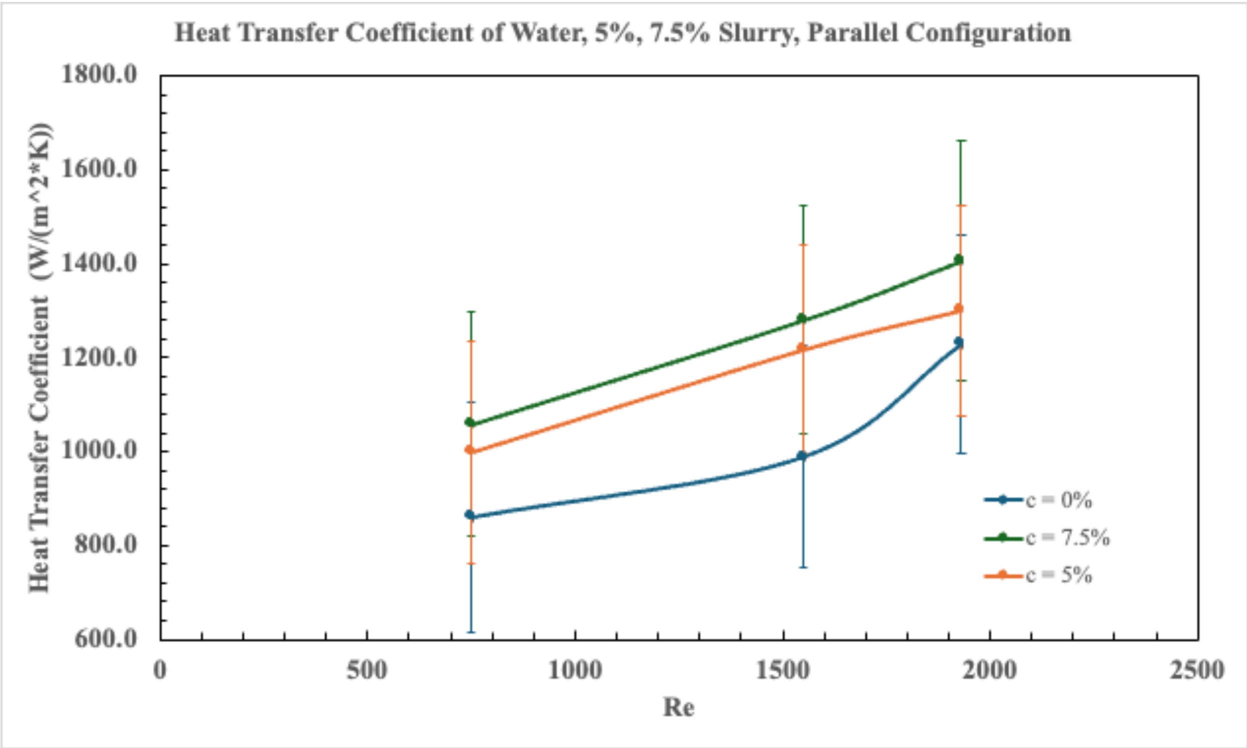

Figure 4.1 Heat transfer coefficient of slurry at c = 0%, 5% and 7.5%, parallel configuration

Among all slurry inlet flow rate conditions, the average heat transfer coefficient was calculated for each slurry concentration at 40°C for both configurations. The average HTC for pure water is 1,026.4 $\frac{W}{m^2K}$, 1172.5 $\frac{W}{m^2K}$ for 5% PCM slurry, and 1,248.3 $\frac{W}{m^2K}$ for 7.5% PCM slurry at T = 40°C on the inlet of the hot water side. This represents a 14.2% and 21.6% improvement from water for 5% PCM and 7.5% PCM respectively with parallel configuration. Figure 4.2 shows the heat transfer coefficients for the same conditions under counterflow.

Figure 4.2 Heat transfer coefficient of slurry at c = 0%, 5% and 7.5%, counterflow configuration

The average heat transfer coefficient is 1064.9 $\frac{W}{m^2K}$ for plain water in this configuration. Here, the average heat transfer coefficients are 1,243.0 $\frac{W}{m^2K}$ and 1,291.0 $\frac{W}{m^2K}$ for c = 5% and c = 7.5%, respectively. This represents a 16.7% improvement and 21.2% improvement over water in the counterflow configuration. Both 5% and 7.5% MEPCM slurry show significant gains regardless of configuration, with 7.5% MPCM having the most improvement over plain water. These results indicate that as particle concentration increases, the heat transfer coefficient also increases. Improvement in heat transfer performance is due to the increase in latent heat absorption available by the increased particle concentration, increasing the heat transfer dissipation rate, and thereby the heat transfer coefficient. The addition of the particles increases the specific heat capacity of the fluid, enhancing the heat transfer rate of the slurry and heat exchanger. Additionally, as Re increases for each respective mass fraction, the heat transfer rate is also shown to increase. As the Reynolds number increases, mixing and convective energy transport increases, resulting in a higher heat dissipation rate from the hot water.

4.2 Pressure Drop

Figure 4.3 represents the comparison of all three compositions with respect to Reynolds number. It can be seen that the pressure drops increases along with the increase in Reynolds. Additionally, pressure drop increases with concentration of MPCM. With respect to the baseline, the pressure drops increased by 112.6% and 125.8% for 5% MPCM slurry for Re = 1550 and Re = 1930. Similarly, the pressure drops increase by 321.2% and 288.1% over baseline for 7.5% MPCM for Re = 1550 and Re = 1930.

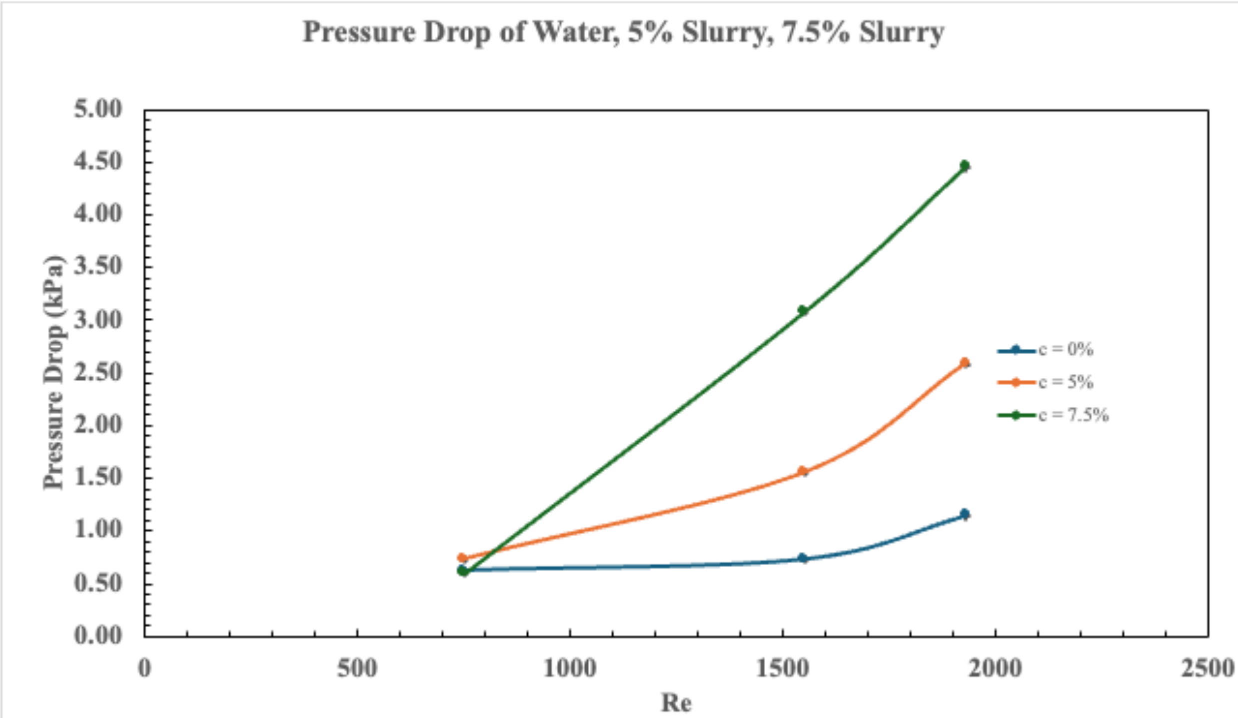

Figure 4.3 Average pressure drop across heat exchanger for c = 0%, 5% and 7.5%

As the particle concentration increases, the viscosity of the slurry also increases. The particles have a large surface area to volume ratio, leading to an increase in viscosity. It can be noted that the average viscosity of 5% MPCM slurry is 30.9% higher than that of water, and the average viscosity of 7.5% MPCM slurry is 44.5% higher than that of water for shear rates of 0-200 s^{-1}. As the viscosity of the fluid increases, flow resistance is greater, and a higher pressure differential is required for the fluid to flow. This results in higher pumping power requirements, which can negate the positive effects of the increased heat transfer rate as seen in Figure 4.1. Additionally, the pressure drop increases exponentially with an increase in Reynolds number for both 5% and 7.5% MPCM slurry.

4.3 Effective Heat Capacity and PCM Concentration

Figure 4.4 shows the effective heat capacity of the slurries based on the measured heat loss (Q) and the difference in slurry inlet and outlet conditions. The average heat capacity of the baseline (c = 0%) is 4,595.1 $\frac{J}{kg*K}$, or 9.8% above the known heat capacity of pure water, which is 4,184 $\frac{J}{kg*K}$. The heat capacity of 5% MPCM averages to 5,382.5 $\frac{J}{kg*K}$, 28.7% above the known heat capacity of pure water and 17.1% above the value measured from this set of experiments. The average effective heat capacity of 7.5% MPCM slurry is 7,429.7$\frac{J}{kg*K}$, 77.6% above the theoretical heat capacity of water, and 61.7% above the measured experimental results.

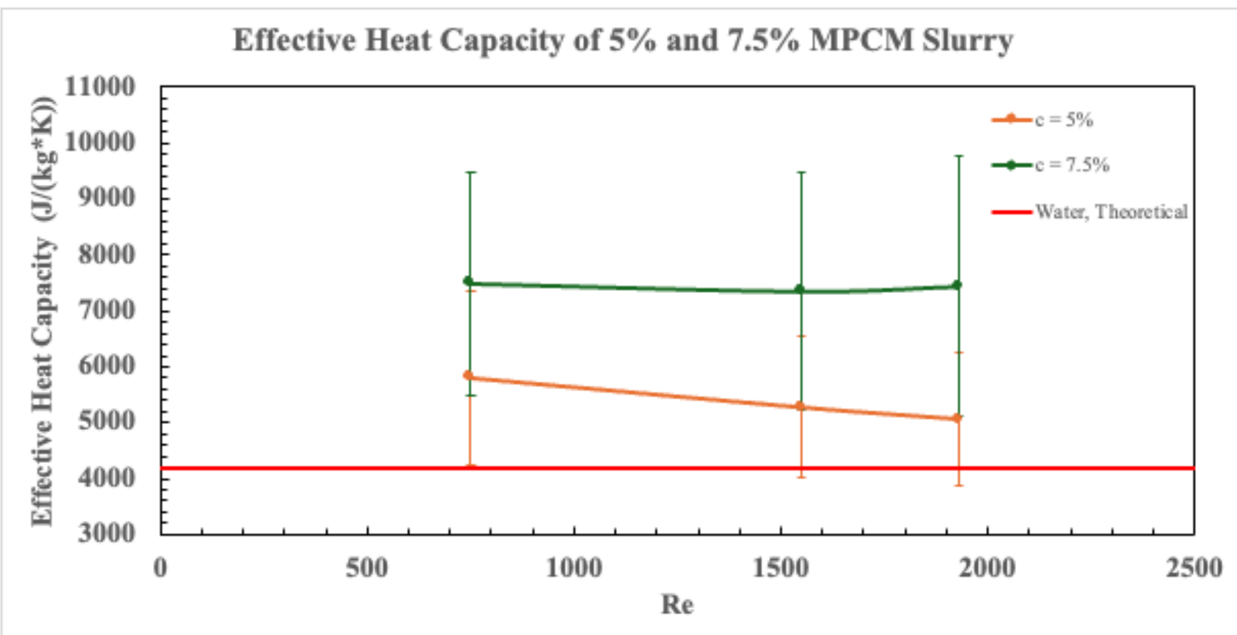

Figure 4.4 Effective heat capacity at c = 5% and 7.5%

The increase in specific heat capacity can be attributed to the latent heat from the particles. When the particles melt, the effective specific heat of the slurry becomes higher, and the heat dissipation rate increases, resulting in better heat transfer. As seen in Figure 4.1 and Figure 4.2, the 7.5% MPCM slurry demonstrates the best heat transfer performance.

4.4 Performance Enhancement Criteria

As demonstrated in these results, 5% and 7.5% MPCM slurries offer significant heat transfer improvements over water. The PEC was used to compare the benefits from the improved heat transfer performance of the slurries with the costs from higher pumping power associated with the increased pressure drop, when compared to water. The PEC against slurry mass fraction is shown in Figure 4.5.

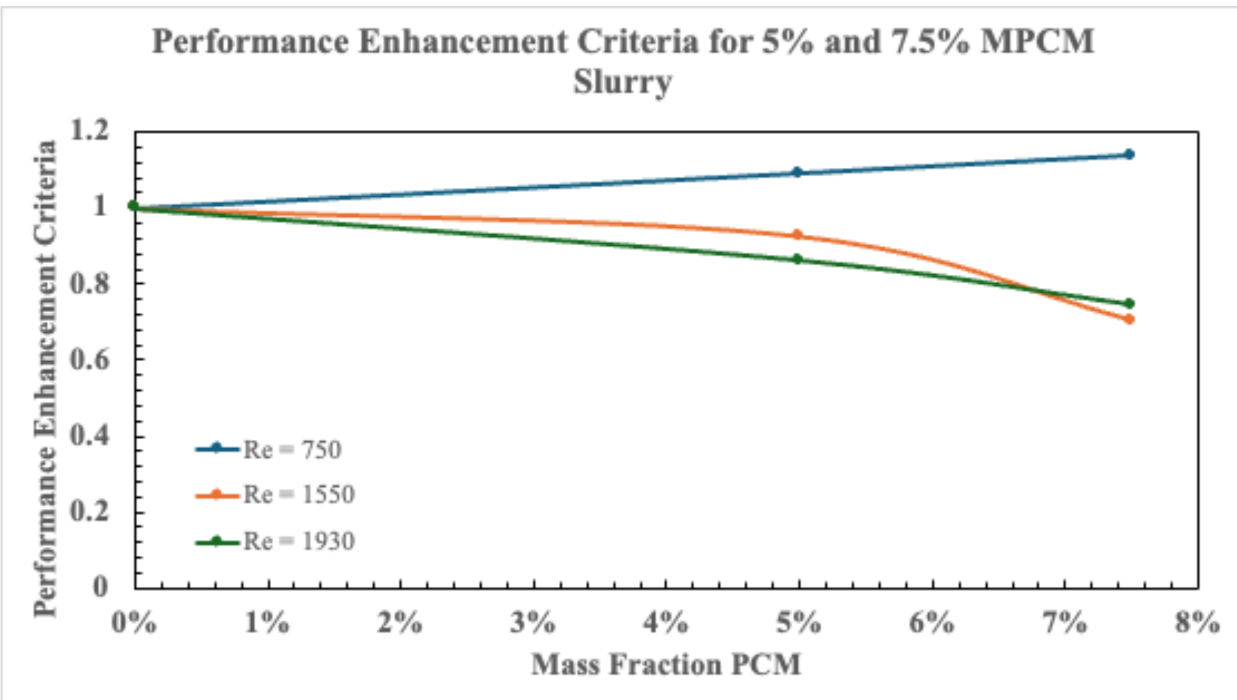

Figure 4.5 Performance Enhancement Criteria of 5% and 7.5% MPCM slurry

At Re = 750, the performance of 5% MPCM and 7.5% MPCM are comparable. However, at Re = 1550, the average PEC of 5% MPCM is 0.93 compared to 0.70 for 7.5% MPCM, indicating a 31.8% decrease in the PEC for the higher concentration of slurry across both configurations of the heat exchanger. At Re = 1930, the average PEC of 5% MPCM is 0.86 compared to 0.74 for 7.5% MPCM, representing a 15.9% decrease in PEC. Additionally, the PEC is only >1 in the case of Re = 750. For both Re = 1550 and Re = 1930, the PEC is < 1, indicating that water has superior thermo-hydraulic performance. The heat transfer coefficient for 5% and 7.5% MPCM slurry is significantly higher than that of water at Re > 1550, however, the difference in the pressure drop increases exponentially past Re = 750, as shown in Figure 4.3, especially for 7.5% MPCM slurry. These results show that a low Re is preferred, as it provides a longer residence time for more complete PCM melting. Though heat dissipation is significantly improved at Re > 750 due to convection, the pressure drop increases at a rate that outweighs the benefits in heat transfer performance, resulting in a suboptimal PEC. Additionally, the residence time is reduced, which means that the particles may not be fully melted, causing heat transfer improvements to be outweighed by the increase in pressure drop.

Chapter 5 Conclusions and Recommendations

The investigation in this thesis presents the thermal, rheological, and stability characterization of MPCS consisting of Nextek 37D and water, along with an evaluation of the use of this MPCS in a shell-and-tube heat exchanger. The results of the experiment show how the properties of the MEPCM improve the heat transfer capacity of the working fluid, and thereby the heat transfer performance within the heat exchanger. The key conclusions from this study are summarized below:

1. The experimental study examined the effects of particle mass concentration on the heat transfer performance of MPCS. For parallel flow, the average heat transfer coefficient for pure water measured was 1,026 $\frac{W}{m^2K}$ compared to 1,172.4 $\frac{W}{m^2K}$ (14.2% increase) for 5% MPCM slurry, and 1,248.3 $\frac{W}{m^2K}$ (21.6% increase) for 7.5% MPCM slurry. For counterflow, the average heat transfer coefficient for pure water was measured as 1,064.9 $\frac{W}{m^2K}$, compared to 1,243.0 $\frac{W}{m^2K}$ (16.7% increase) and 1,291.0 $\frac{W}{m^2K}$ (21.2% increase) for 5% and 7.5% MPCM slurry respectively. Increasing particle mass concentration in the slurry has positive effects on the heat transfer performance.
2. Increasing particle concentration in the MPCM slurry leads to an increase in specific heat capacity of the working fluid when the particles are in the melting range. The average effective heat capacity of 5% and 7.5% MPCM slurry were 28.7% and 77.6% above the heat capacity of water. As particle concentration increases, the amount of latent heat that can be absorbed by the slurry is also greater as the particles melt. This increase in effective heat capacity results in the heat transfer performance gains compared to the baseline, as the

maximum heat transfer rate from water increases. Additionally, the effectiveness of the heat exchanger also increases.

3. Increasing particle concentration in MPCS also results in an increase in pressure drop. Pressure drop across the heat exchanger increased by as much as 125.8% and 321.2% in 5% MPCM and 7.5% MPCM slurry compared to water. The increase in pressure drop can be attributed to the increase in viscosity as particle concentration becomes higher. On average, the viscosity of 5% MPCM and 7.5% MPCM slurry was measured to be 30.9% and 44.5% higher than that of water. The increase in pressure drop results in higher pumping power requirements.
4. At Re > 1550, the PEC of 5% MPCM slurry is greater than the performance enhancement criterion (PEC) of 7.5% MPCM slurry. Though 7.5% MPCM slurry had significantly higher heat transfer performance compared to 5% MPCM slurry, the pressure drop and friction losses were also significant. For this reason, 5% MPCM has superior thermo-hydraulic performance.
5. This study has established the benefit of using MPCM-water slurry in a shell-and-tube heat exchanger. Future development of this study could focus on the addition of other hot-side inlet temperatures to determine the effectiveness of MPCM slurry in various operating regimes. Furthermore, the use of MPCM with other heat exchanger geometries and base fluids, such as microchannels and dielectric fluids could provide insight on the usefulness of MPCM more specifically to electronics thermal management applications.

Bibliography

[1] A. Sharma, V. V. Tyagi, C. R. Chen, and D. Buddhi, "Review on thermal energy storage with phase change materials and applications," *Renew. Sustain. Energy Rev.*, vol. 13, no. 2, pp. 318–345, Feb. 2009, doi: 10.1016/j.rser.2007.10.005.

[2] M. M. Farid, A. M. Khudhair, S. A. K. Razack, and S. Al-Hallaj, "A review on phase change energy storage: materials and applications," *Energy Convers. Manag.*, vol. 45, no. 9, pp. 1597–1615, Jun. 2004, doi: 10.1016/j.enconman.2003.09.015.

[3] R. Kandasamy, X.-Q. Wang, and A. S. Mujumdar, "Application of phase change materials in thermal management of electronics," *Appl. Therm. Eng.*, vol. 27, no. 17–18, pp. 2822–2832, Dec. 2007, doi: 10.1016/j.applthermaleng.2006.12.013.

[4] H. Mehling and L. F. Cabeza, "Solid-liquid phase change materials," in *Heat and cold storage with PCM: An up to date introduction into basics and applications*, H. Mehling and L. F. Cabeza, Eds., Berlin, Heidelberg: Springer, 2008, pp. 11–55. doi: 10.1007/978-3-540-68557-9_2.

[5] J. Wei, Z. Li, L. Liu, and X. Liu, "Preparation and characterization of novel polyamide paraffin MEPCM by interfacial polymerization technique," *J. Appl. Polym. Sci.*, vol. 127, no. 6, pp. 4588–4593, 2013, doi: 10.1002/app.37681.

[6] K. Ghasemi, S. Tasnim, and S. Mahmud, "PCM, nano/microencapsulation and slurries: A review of fundamentals, categories, fabrication, numerical models and applications," *Sustain. Energy Technol. Assess.*, vol. 52, p. 102084, Aug. 2022, doi: 10.1016/j.seta.2022.102084.

[7] P. Zhang, Z. W. Ma, and R. Z. Wang, "An overview of phase change material slurries: MPCS and CHS," *Renew. Sustain. Energy Rev.*, vol. 14, no. 2, pp. 598–614, Feb. 2010, doi: 10.1016/j.rser.2009.08.015.

[8] K. E. Kasza and M. M. Chen, "Improvement of the Performance of Solar Energy or Waste Heat Utilization Systems by Using Phase-Change Slurry as an Enhanced Heat-Transfer Storage Fluid," *J. Sol. Energy Eng.*, vol. 107, no. 3, pp. 229–236, Aug. 1985, doi: 10.1115/1.3267683.

[9] J. L. Alvarado, C. Marsh, C. Sohn, G. Phetteplace, and T. Newell, “Thermal performance of microencapsulated phase change material slurry in turbulent flow under constant heat flux,” *Int. J. Heat Mass Transf.*, vol. 50, no. 9–10, pp. 1938–1952, May 2007, doi: 10.1016/j.ijheatmasstransfer.2006.09.026.

[10] P. Charunyakorn, S. Sengupta, and S. K. Roy, “Forced convection heat transfer in microencapsulated phase change material slurries: flow in circular ducts,” *Int. J. Heat Mass Transf.*, vol. 34, no. 3, pp. 819–833, Mar. 1991, doi: 10.1016/0017-9310(91)90128-2.

[11] X. Wang *et al.*, “Heat transfer of microencapsulated PCM slurry flow in a circular tube,” *AIChE J.*, vol. 54, no. 4, pp. 1110–1120, 2008, doi: 10.1002/aic.11431.

[12] Z. Zhao, R. Hao, and Y. Shi, “Parametric Analysis of Enhanced Heat Transfer for Laminar Flow of Microencapsulated Phase Change Suspension in a Circular Tube with Constant Wall Temperature,” *Heat Transf. Eng.*, vol. 29, no. 1, pp. 97–106, Jan. 2008, doi: 10.1080/01457630701677631.

[13] R. Shaukat, A. Qamar, Z. Anwar, S. Imran, and M. Amjad, “Experimental Study on Heat Transfer Performance of Mpcm Slurry Flow in Microchannels,” *SSRN Electron. J.*, Jan. 2022, doi: 10.2139/ssrn.4073146.

[14] S. Kuravi, J. Du, and L. C. Chow, “Encapsulated Phase Change Material Slurry Flow in Manifold Microchannels,” *J. Thermophys. Heat Transf.*, vol. 24, no. 2, pp. 364–373, Apr. 2010, doi: 10.2514/1.44276.

[15] I. J. of S. R. in S. and T. Ijsrst, “A Review on Study of Shell and Tube Heat Exchanger,” *Int. J. Sci. Res. Sci. Technol.*, Jan. 2022, doi: 10.32628/IJSRST229218.

[16] E. C. Okonkwo, I. Wole-Osho, I. W. Almanassra, Y. M. Abdullatif, and T. Al-Ansari, “An updated review of nanofluids in various heat transfer devices,” *J. Therm. Anal. Calorim.*, vol. 145, no. 6, pp. 2817–2872, Sep. 2021, doi: 10.1007/s10973-020-09760-2.

[17] K. Mohammadi, W. Heidemann, and H. Müller-Steinhagen, “Numerical Investigation of the Effect of Baffle Orientation on Heat Transfer and Pressure Drop in a Shell and Tube Heat Exchanger With Leakage Flows,” *Heat Transf. Eng.*, vol. 30, no. 14, pp. 1123–1135, Dec. 2009, doi: 10.1080/01457630902972694.

[18] R. Mukherjee, “Effectively Design Shell-and-Tube Heat Exchangers,” *Chem. Eng. Prog.*, 1998.

[19] T. B. Ashagre and D. Rakshit, “Study on flow and heat transfer characteristics of Encapsulated Phase Change Material (EPCM) slurry in Double-Pipe Heat Exchanger,” *J. Energy Storage*, vol. 46, p. 103931, Feb. 2022, doi: 10.1016/j.est.2021.103931.

[20] A. Safari, R. Saidur, F. A. Sulaiman, Y. Xu, and J. Dong, “A review on supercooling of Phase Change Materials in thermal energy storage systems,” *Renew. Sustain. Energy Rev.*, vol. 70, pp. 905–919, Apr. 2017, doi: 10.1016/j.rser.2016.11.272.

[21] M. Chen, Y. Wang, and Z. Liu, “Experimental study on micro-encapsulated phase change material slurry flowing in straight and wavy microchannels,” *Appl. Therm. Eng.*, vol. 190, p. 116841, May 2021, doi: 10.1016/j.applthermaleng.2021.116841.

[22] I. Shamseddine, F. Pennec, P. Biwole, and F. Fardoun, “Supercooling of phase change materials: A review,” *Renew. Sustain. Energy Rev.*, vol. 158, p. 112172, Apr. 2022, doi: 10.1016/j.rser.2022.112172.

[23] M. Delgado, A. Lázaro, C. Peñalosa, and B. Zalba, “Experimental analysis of the influence of microcapsule mass fraction on the thermal and rheological behavior of a PCM slurry,” *Appl. Therm. Eng.*, vol. 63, no. 1, pp. 11–22, Feb. 2014, doi: 10.1016/j.applthermaleng.2013.10.011.

[24] G. H. Zhang and C. Y. Zhao, “Thermal and rheological properties of microencapsulated phase change materials,” *Renew. Energy*, vol. 36, no. 11, pp. 2959–2966, Nov. 2011, doi: 10.1016/j.renene.2011.04.002.

[25] Ir. R. Rutgers, “Relative viscosity of suspensions of rigid spheres in Newtonian liquids,” *Rheol. Acta*, vol. 2, no. 3, pp. 202–210, Sep. 1962, doi: 10.1007/BF01983952.

[26] K. Dutkowski and J. J. Fiuk, “Experimental research of viscosity of microencapsulated PCM slurry at the phase change temperature,” *Int. J. Heat Mass Transf.*, vol. 134, pp. 1209–1217, May 2019, doi: 10.1016/j.ijheatmasstransfer.2019.02.036.

[27] R. Deepak Selvakumar and S. Dhinakaran, “Effective viscosity of nanofluids — A modified Krieger–Dougherty model based on particle size distribution (PSD) analysis,” *J. Mol. Liq.*, vol. 225, pp. 20–27, Jan. 2017, doi: 10.1016/j.molliq.2016.10.137.

[28] X. Wang *et al.*, “Flow and heat transfer behaviors of phase change material slurries in a horizontal circular tube,” *Int. J. Heat Mass Transf.*, vol. 50, no. 13–14, pp. 2480–2491, Jul. 2007, doi: 10.1016/j.ijheatmasstransfer.2006.12.024.

[29] V. Vand, “Theory of Viscosity of Concentrated Suspensions,” *Nature*, vol. 155, no. 3934, pp. 364–365, Mar. 1945, doi: 10.1038/155364b0.

[30] J. C. Mulligan, D. P. Colvin, and Y. G. Bryant, “Microencapsulated phase-change material suspensions for heat transfer in spacecraft thermal systems,” *J. Spacecr. Rockets*, May 2012, doi: 10.2514/3.26753.

[31] M. M. Robins, “Emulsions — creaming phenomena,” *Curr. Opin. Colloid Interface Sci.*, vol. 5, no. 5, pp. 265–272, Nov. 2000, doi: 10.1016/S1359-0294(00)00065-0.

[32] M. Delgado, A. Lázaro, J. Mazo, and B. Zalba, “Review on phase change material emulsions and microencapsulated phase change material slurries: Materials, heat transfer studies and applications,” *Renew. Sustain. Energy Rev.*, vol. 16, no. 1, pp. 253–273, Jan. 2012, doi: 10.1016/j.rser.2011.07.152.

[33] Y. Konuklu, H. O. Paksoy, M. Unal, and S. Konuklu, “Microencapsulation of a fatty acid with Poly(melamine–urea–formaldehyde),” *Energy Convers. Manag.*, vol. 80, pp. 382–390, Apr. 2014, doi: 10.1016/j.enconman.2014.01.042.

[34] Z. Lin, Z. Wei, L. Shuang, and J. Xiangyu, “Experimental study on improving stability of PCM and MEPCM slurry with different surfactants,” *Int. J. Low-Carbon Technol.*, vol. 13, no. 3, pp. 272–276, Sep. 2018, doi: 10.1093/ijlct/cty027.

[35] T. B. Ashagre and D. Rakshit, “Study on flow and heat transfer characteristics of Encapsulated Phase Change Material (EPCM) slurry in Double-Pipe Heat Exchanger,” *J. Energy Storage*, vol. 46, p. 103931, Feb. 2022, doi: 10.1016/j.est.2021.103931.

[36] J. L. Alvarado, C. Marsh, C. Sohn, G. Phetteplace, and T. Newell, “Thermal performance of microencapsulated phase change material slurry in turbulent flow under constant heat flux,” *Int. J. Heat Mass Transf.*, vol. 50, no. 9, pp. 1938–1952, May 2007, doi: 10.1016/j.ijheatmasstransfer.2006.09.026.

[37] S. A. Marzouk, M. M. Abou Al-Sood, M. K. El-Fakharany, and E. M. S. El-Said, “Thermo-hydraulic study in a shell and tube heat exchanger using rod inserts consisting of wire-nails with air injection: Experimental study,” *Int. J. Therm. Sci.*, vol. 161, p. 106742, Mar. 2021, doi: 10.1016/j.ijthermalsci.2020.106742.

[38] D. L. Gee and R. L. Webb, “Forced convection heat transfer in helically rib-roughened tubes,” *Int. J. Heat Mass Transf.*, vol. 23, no. 8, pp. 1127–1136, Aug. 1980, doi: 10.1016/0017-9310(80)90177-5.